confirms the scheme through reactions 1-4 and the assignments of transient spectra.

The quenching rate constant of triplet benzophenone by TBPOH in benzene is slightly smaller than the diffusion-controlled rate.[26] Das et al.[17] reported quenching rate constants by several substituted and nonsubstituted phenols. The quenching rate by nonsubstituted phenol seems to be a limit of the diffusion controlled, as seen in Table II. The smaller value for TBPOH would be caused by obstruction of approach of triplet benzophenone by the bulky *tert*-butyl groups and reduction of the Arrhenius factor.

In the red region we detected the buildup signals appearing with the same kinetics at 400 nm. Since benzophenone ketyl radical has no absorption in the region between 600 and 700 nm as seen in Figure 2 and at 500 ns after the laser irradiation triplet benzophenone is completely quenched, the transient spectrum at 700 ns in the red region is attributed to the phenoxy radical.

In this time range, there was no appreciable decay of both the ketyl and phenoxy radicals and the concentrations of these radicals should be equal to each other. The ratio of the extinction coefficient of the phenoxy radical to that of the ketyl radical, therefore, is represented by the ratio of absorbances of these transients. Using the value 3300 M^{-1} cm^{-1} of the extinction coefficient of the ketyl radical at 540 nm, we determined the extinction coefficient of the phenoxy radical at 670 nm to be 1200 M^{-1} cm^{-1}. Chang et al.[27] carried out CNDO/S calculations of aromatic radicals and predicted that the n-π^* transition of nonsubstituted phenoxy radical lay lower than 25000 cm^{-1}. Ward[14] assigned the red absorption to the n-π^* transition. In the case of thiophenoxy radical, Jinguji et al.[8] reported the absorption maximum of 590 nm by the laser-induced emission and tentatively assigned it to the n-π^* transition. The rather low extinction coefficient in this study suggests the n-π^* character of the red absorption though the value of 1200 M^{-1} cm^{-1} seems to be slightly large for the pure n-π^* transition.

Registry No. BP, 119-61-9; TBPOH, 732-26-3; BPH, 16592-08-8; TBPO, 2525-39-5.

(26) Birks, J. B.; Dyson, D. J.; Munro, I. H. *Proc. R. Soc. London, A* **1963**, *275*, 575.

(27) Chang, H. M.; Jaffe, H. H.; Masmanidis, C. A. *J. Phys. Chem.* **1975**, *79*, 1118.

One-Photon Infrared Photodissociation of Polyatomic Ions in a Fast Beam

M. J. Coggiola,* P. C. Cosby, H. Helm, J. R. Peterson,

Molecular Physics Laboratory, SRI International, Menlo Park, California 94025

and Robert C. Dunbar†

Chemistry Department, Case Western Reserve University, Cleveland, Ohio 44106 *(Received: August 13, 1986; In Final Form: January 21, 1987)*

Photodissociation of 22 vibrationally excited polyatomic ions, ranging in size from four to thirteen atoms, has been observed following absorption of a single CO_2-laser photon. In a number of cases the infrared wavelength dependence of the process shows well-defined peaking, which can be interpreted as absorption at the normal-mode frequencies of the ion. Kinetic energy release and order-of-magnitude fragmentation rate information have also been obtained for both photon-induced and metastable decomposition of a number of the ions. RRKM theory modeling indicates that these data are compatible with a quasi-equilibrium theory description of the unimolecular decomposition of highly vibrationally excited molecular ions. Considered as resulting from the last photon absorption of a multiphoton dissociation process, these results are relevant to understanding infrared multiphoton photochemistry of polyatomic molecules.

Introduction

In its early stages, the investigation of multiphoton excitation and multiphoton dissociation (MPD) was confined to studies of molecules that were initially in their ground electronic state and vibrationally cool. These conditions were especially enhanced in those experiments which utilized a thermal energy neutral molecular beam formed by supersonic expansion.[1] While these experiments continue to provide a great deal of insight into the dynamics of MPD, a new class of experiments has appeared recently involving infrared absorption by initially excited species. These experiments have employed a number of excitation techniques and have probed a wide range of initial excitation. For example, Welge and co-workers first observed the MPD of a vibrationally hot SF_5^+ ion beam produced in a plasma source.[2] They were subsequently able to measure the lifetime distribution of the dissociating ions using a time-of-flight method.[3] An RRKM analysis of the results showed that the majority of ions absorbed 4-6 photons in excess of the dissociation energy. In a later experiment, the same group studied the MPD of NO_2 which was initially excited by a one-photon visible absorption.[4] Although the visible photon supplied >90% of the dissociation energy and only 2-3 infrared photons (10 μm) were needed to observe product NO formation, they found the dissociation to be very fast and fully consistent with a statistical description. Several variations of this visible + IR dissociation scheme have also been reported recently. Heller and West[5] prepared vibrationally hot CrO_2Cl_2 molecules via a nonradiative decay following visible excitation from the ground state. Subsequent multiphoton IR absorption was found to be efficient, even off resonance, as might be expected for molecules initially in the quasi-continuum. Even in the presence of competing relaxation processes (V-V, V-T), they found that efficient IR absorption persisted. A similar sequence of visible (electronic) excitation followed by internal conversion to a vi-

† John Simon Guggenheim Fellow, 1978-79.

(1) Schulz, P. A.; Sudbø, Aa. S.; Kranovich, D. J.; Kwok, H. S.; Shen, Y. R.; Lee, Y. T. *Annu. Rev. Phys. Chem.* **1979**, *30*, 379.
(2) von Hellfeld, A.; Feldman, D.; Welge, K. H.; Fournier, A. P. *Opt. Commun.* **1979**, *30*, 193.
(3) von Hellfeld, A.; Anndt, B.; Feldman, D.; Fournier, A. P.; Welge, K. H. *Appl. Phys.* **1980**, *21*, 9.
(4) Feldman, D.; Zacharias, H.; Welge, K. H. *Chem. Phys. Lett.* **1980**, *69*, 466.
(5) Heller, D. F.; West, G. A. *Chem. Phys. Lett.* **1980**, *69*, 419.

0022-3654/87/2091-2794$01.50/0

brationally excited ground electronic state which leads to enhanced IR MPD has also been observed in $C_6H_5CN^+$ stored in an ICR (ion cyclotron resonance) trap.[6] Dunbar and co-workers[7] have measured significant increases in the rate of visible two-photon dissociation of ICR trapped ions that are simultaneously irradiated with a low-power ($\sim$10 W/cm^2) CW CO_2 laser. Finally, Barfknecht and Brauman[8] have recently shown a clear example of IR MPD of vibrationally excited electronic-ground-state molecular ions.

While each of these experiments prepared an initially excited population of neutral or ionic molecules, they all required the absorption of several photons to yield products. In contrast, we have reported[9] on the collision free photodissociation of a fast beam of CF_3X^+ (X = I, Br, Cl) ions using a CW CO_2 laser. Since the conditions of the experiment were such that absorption of more than one infrared photon by a given ion was vanishingly improbable, this observation was interpreted as resulting from the single-photon photodissociation of internally excited ions lying very near the dissociation threshold.

That study showed for the first time that such a one-photon dissociation process can exhibit a marked wavelength dependence. Specifically, for CF_3I^+ formed by electron impact, a sharp peak in the CF_3^+ photofragment yield was found at $\sim$950 cm^{-1} and was associated with absorption by the ν_1 mode of the ion. In addition, a smaller (2–3%) peak near 1080 cm^{-1} was also found. Both the linear power dependence and the measured small ($\ll h\nu$) kinetic energy release of the fragments were consistent with the single-photon mechanism. A subsequent study by Thorne and Beauchamp[10] of the same CF_3I^+ photodissociation in an ICR trap using both CW and pulsed CO_2 lasers confirmed this wavelength selectivity. Since the degree of vibrational excitation present in their ions at the time of absorption is not known, the number of photons required for dissociation could not be determined. Nonetheless, a very large (60%) CF_3^+ fragment yield peaking near 960 cm^{-1} was found and attributed to absorption involving the ν_1 vibrational mode of ions initially in the excited $X^2E_{1/2}$ state.

More recently, Jarrold et al.[11] have reported on the photodissociation of vibrationally excited CF_3I^+ and CF_3Br^+ by a single infrared photon in the second field-free region of a double focusing mass spectrometer. Again, that study confirmed the strong wavelength dependence of the infrared absorption and dissociation of these ions. Using a variety of evidence, Jarrold et al.[11] concluded that the strong absorption centered at 946 cm^{-1} was correctly associated with the ν_1 mode of the $X^2E_{1/2}$. In addition, they concluded that the smaller secondary peak found in both our original study[9] and their later study[11] was due to the ν_4 C–F antisymmetric stretch.

Jarrold et al.[11] also reported average kinetic energy release values for both CF_3I^+ and CF_3Br^+ as a function of the ion source temperature. Values for both ions were in the range of 17–19 meV, and nearly constant with source temperature, although the actual kinetic energy release distributions broadened with increasing temperature. Calculations using a statistical phase space model were able to reproduce the measured kinetic energy distributions, thus indicating that the energy release was essentially statistical.

In a continuation of these experiments, we have observed the single-photon IR dissociation of a large number of vibrationally excited molecular ions in a fast beam. In addition to measuring the wavelength dependence of the absorption, we have also determined the kinetic energy release accompanying dissociation as well as obtaining an estimate of the dissociative lifetime for several ions. Considered as being equivalent to the action of the *last* photon in a multiphoton infrared photodissociation sequence, this experiment has special interest because it provides a specific probe of this one step in the complex multiphoton photochemical process. Determination of the dissociation lifetimes, kinetic energy releases, and wavelength dependences for a wide variety of cases gives insight into the nature of the dissociation process and into the photophysical properties of highly excited molecules. In addition, these more complete measurements allow for the application of RRKM theory to the dissociation of these polyatomic molecular ions.

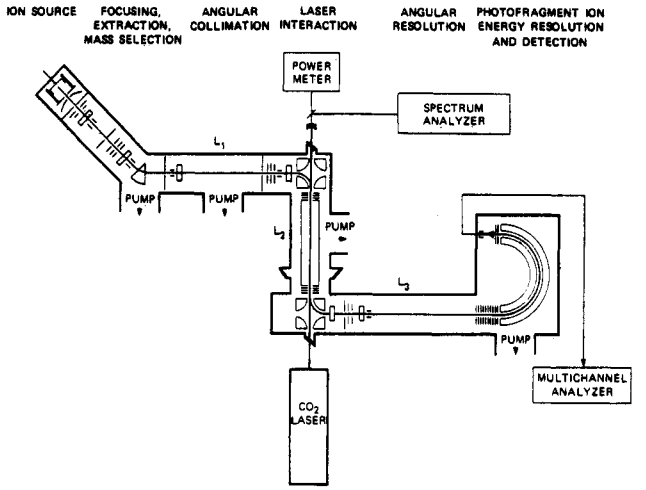

Figure 1. Schematic diagram of the SRI laser–ion coaxial beams spectrometer used for these infrared photodissociation studies. Ion flight path lengths L_{1-3} are measured along the straight-line trajectories indicated.

Experimental Section

All measurements reported here were made using the same laser–ion coaxial beams spectrometer used and described previously,[9,12] and shown schematically in Figure 1. Briefly, ions formed in the pure parent gas by electron impact at 100 eV are extracted and accelerated to a final kinetic energy of 2–4 keV. The magnetically mass-selected ion beam was electrostatically deflected by 90° and merged with the output from a line-tunable CW CO_2 laser (Advanced Kinetics MIRL-50). The laser beam was collimated to 3 mm diameter and overlapped the ion beam for a distance of $\sim$33 cm before an electrostatic quadrupole deflected the ions by 90°. This quadrupole could be tuned to pass either the parent ions, or fragment ions formed within the interaction region. The transmitted laser power was generally 0.5–4.0 W at P(16) in a TEM_{00} mode unfocussed. A grating spectrum analyzer was used to determine the laser wavelength. The laboratory kinetic energies of fragment ions were determined by using a 180° hemispherical electrostatic analyzer. This energy analysis serves to identify uniquely the masses of the fragment ions. Further, an analysis of the measured laboratory kinetic energy distribution yields the center-of-mass kinetic energy release distribution which results from the dissociation process.[13]

In addition to absorption-induced dissociation, ion fragmentation can also arise from collision-induced dissociation (CID) and dissociation of metastable parent ions, i.e., ions formed in the source with total internal energy greater than the lowest dissociation energy, which undergo spontaneous unimolecular dissociation within the region of observation. These two processes were distinguished from the dissociation mechanism by modulating the photon beam and using synchronous detection methods. It is further possible to separate CID from spontaneous metastable dissociation as the former is pressure dependent while the latter is not.

(6) Wight, C. A.; Beauchamp, J. L. *Chem. Phys. Lett.* **1981**, *77*, 30.
(7) Dunbar, R. C.; Hays, J. D.; Hanovich, J. P.; Lev, N. B. *J. Am. Chem. Soc.* **1980**, *102*, 3950. Honovich, J. P.; Dunbar, R. C. *J. Am. Chem. Soc.* **1982**, *104*, 6220. Honovich, J. P.; Dunbar, R. C. *J. Phys. Chem.* **1983**, *87*, 3755.
(8) Barfknecht, A. T.; Brauman, J. I. *J. Phys. Chem.* **1986**, *84*, 3870.
(9) Coggiola, M. J.; Cosby, P. C.; Peterson, J. R. *J. Chem. Phys.* **1980**, *72*, 6507.
(10) Thorne, L. R.; Beauchamp, J. L. *J. Chem. Phys.* **1981**, *74*, 5100.
(11) Jarrold, M. F.; Illes, A. J.; Kirchner, N. J.; Wagner-Redeker, W.; Bowers, M. T.; Mandich, M. L.; Beauchamp, J. L. *J. Phys. Chem.* **1983**, *87*, 2213.
(12) Huber, B. A.; Miller, T. M.; Cosby, P. C.; Zeman, H. D.; Leon, R. L.; Moseley, J. T.; Peterson, J. R. *Rev. Sci. Instrum.* **1977**, *48*, 1306.
(13) Holmes, J. L.; Osbone, A. D. *Int. J. Mass. Spectrom. Ion. Phys.* **1977**, *23*, 189.

TABLE I: Experimental Values for Ion Dissociative Energy Release ($\bar{W}$); Fragmentation Ratio (R_3/R_2) (See Text); Lifetime (τ); Cross Section (σ); and Photofragment Wavelength Dependence (λ) for All Ions Studied

	metastable decompn			collision-induced decompn	IR-induced decompn				
	$\bar{W}_{meta}(L_2)^{a,b}$	(R_3/R_2)	$\tau_{meta}{}^c$	$\bar{W}_{CID}{}^b$	$\sigma_{IR}{}^d$	$\lambda_{peak}{}^e$	$\bar{W}_{IR}(L_2)^{a,b}$	(R_3/R_2)	$\tau_{IR}{}^c$
$CF_3I^+ \rightarrow CF_3^+$	*f*			1.2	4.1	947	12	~0	≪1
$CF_3I^+ \rightarrow I^+$				69					
$CF_3Br^+ \rightarrow CF_3^+$	*f*				>0	953	12		
$CF_3Cl^+ \rightarrow CF_3^+$	*f*				>0	B			
$C_2F_5I^+ \rightarrow C_2F_5^+$	4.5 (0.6)	2.1[g]	26		>0	1080 (Fig. 2)	13	0.08[g]	2.2
$C_2F_5Br^+ \rightarrow C_2F_5^+$	2.9	1.6[h]	30		>0	1080 (Fig. 2)	8.4	0.008[h]	1.3
$C_3F_7I^+ \rightarrow C_3F_7^+$	14.2 (14.7)	3.7[g]	>100		2.4	1010 (Fig. 3)	25 (34)	0.66[g]	5.5
$C_3F_7Br^+ \rightarrow C_3F_7^+$	5.5	1.6[h]	49		>0	1000 (Fig. 3)	13.8 (15)	0.16[h]	4.4
$CF_3CH_2I^+ \rightarrow CF_3CH_2^+$	25				>0	≥1081			
$C_6F_5I^+ \rightarrow C_6F_5^+$	49	2.8[g]	39		>0	B		9.5[g]	>120
$C_6F_5Br^+ \rightarrow C_6F_5^+$	98	1.6[h]	49		>0	B		3.2[g]	16
$C_6F_5Cl^+ \rightarrow C_6F_5^+$	72	2.4[g]	40		>0	B		4.7[g]	24
$C_6F_6^+ \rightarrow C_5F_3^+$	139				>0	B			
$C_6F_6^+ \rightarrow C_5F_4^+$	45				~0				
$C_6F_6^+ \rightarrow C_6F_5^+$	78				~0				
$C_6F_6^+ \rightarrow C_3F_3^+$					~0				
$C_6H_5I^+ \rightarrow C_6H_5^+$	28.5 (27.6)	2.5[h]	>100		0.09	B			
$C_6H_5Br^+ \rightarrow C_6H_5^+$	35.0 (40.2)	2.7[h]	∞						
$C_6H_5CN^+ \rightarrow C_6H_4^+$	35.1 (38.3)	2.3[h]	74		1.2	B			
$CF_3^+ \rightarrow CF_2^{+i}$	*f*				>0	>1073			
$C_2F_5^+ \rightarrow CF_3^{+j}$	~6			~23	>0	1035 (Fig. 4)	15.2		
$C_2F_5^+ \rightarrow CF_3^{+k}$	~6				>0	~1035 (Fig. 4)	14.2		
$C_3F_6^+ \rightarrow C_2F_4^+$	11.9 (12.9)	4.0[g]	∞		>0	1030 (Fig. 5)	14.4	1.6[g]	7.3
$CH_2F^+ \rightarrow CHF^{+l}$	*f*				>0				
$CH_3F^+ \rightarrow CH_2F^+$	88			80	>0	<925			
$CH_3F^+ \rightarrow CHF^+$	~135			~155	~0				
$CH_4F^+ \rightarrow CH_3F^l$	*f*					>0			
$CF_2I^+ \rightarrow I^{+m}$						>0	B	10	

[a] Numbers in parentheses are average kinetic energy releases measured for decompositions in L_3. [b] In millielectronvolts. [c] In microseconds. [d] $\times 10^{-20}$ cm^2. [e] Estimated peak positions given in cm^{-1}; B signifies a broad, essentially featureless spectrum. [f] No metastables observed. [g] L_2 = 34 cm, L_3 = 123 cm. [h] L_2 = 58 cm, L_3 = 129 cm. [i] Formed from CF_3Br. [j] Formed from C_2F_5I. [k] Formed from C_2F_6. [l] Formed from CH_3F. [m] Formed from CF_3I. [n] Results are included for metastable (pressure-independent) dissociation, collision-induced dissociation, and infrared photodissociation.

Information on the dissociative lifetimes of both photoexcited and metastable ions can be obtained by operating the laser–ion spectrometer in two different modes. In the first mode, both the hemispherical electrostatic analyzer and the second quadrupole are tuned to pass only fragment ions of the same energy (and hence the same mass for the monoenergetic ion beam). In this configuration, the detected signal is proportional to the number of fragment ions produced in the region between the two quadrupoles (denoted as L_2). For the second mode, the hemispherical analyzer remains tuned to pass fragment ions, while the second quadrupole is adjusted to pass only parent ions. With this arrangement, the signal arises only from ion fragmentation which occurs along the beam path between the quadrupole and the analyzer (denoted as L_3).

The fragmentation rates (R) were estimated by measuring the amount of dissociation occurring in L_2 and L_3 separately and taking the ratio (R_3/R_2). If (as is actually not the case) the entire population of ions is dissociating unformly at constant rate throughout the traversal of L_2 and L_3, then a fragmentation lifetime τ may be defined, and related to the observed (R_3/R_2) ratio by

$$R_3/R_2 = \frac{[1 - \exp(-t_3\tau^{-1})]\exp(-t_1\tau^{-1})}{1 - \exp(-t_2\tau^{-1})}$$

where t_2 and t_3 are the times spent traversing L_2 and L_3, and t_1 is the time spent in the interval between L_2 and L_3. These "apparent" lifetimes were calculated and are listed in Tables I and II. For the dissociation case, it is even less justifiable to calculate a single lifetime, since not only are ions with differing energy contents dissociating at different rates, but also different ions absorb photons at different points along L_2. Nevertheless, apparent lifetimes were again calculated, assuming photon absorption in the center of L_2 and uniform dissociation. In view of the several assumptions made in deriving these values, the apparent lifetimes should only be regarded as order-of-magnitude indications, rather than as precise or well-defined lifetimes. In spite of the uncertainties involved, these lifetimes are valuable in establishing the appropriate time scale associated with the dissociative processes.

TABLE II: Comparison of Observed and Calculated Values for Dissociative Energy Release (W), Fragmentation Ratio (R_3/R_2), and Lifetime (τ) for both Metastable and Infrared-Photon-Induced Dissociation[a]

	metastable			IR-induced		
	$W_{meta}{}^b$	$(R_3/R_2)_{meta}$	$\tau_{meta}{}^c$	$W_{IR}{}^b$	$(R_3/R_2)_{IR}$	$\tau_{IR}{}^c$
CF_3I^+						
obsd				12	0	0
calcd	*d*	*d*	*d*	14 (9)	~0	≪1
$C_2F_5I^+$						
obsd	4.5	2.1	26	13	0.08	2.2
calcd	~3	2.1	26	12 (9)	0.12	2.8
$C_3F_7I^+$						
obsd	14.2	3.7	>100	25	0.66	5.5
calcd	10 (9)	3.2	170	21 (15)	0.53	5.5

[a] See text for details of the statistical (RRKM) calculations. [b] In millielectronvolts. Energies in parentheses calculated from Klots' expression. [c] In microseconds. See experimental section for discussion of these apparent lifetimes. [d] No metastable decompositions expected.

For several of the ions covered in this study, it was possible to estimate their photodissociation cross sections by direct measurement of the ion beam current in the presence and absence of the laser. The cross sections are calculated from the equation

$$\sigma_{IR} = \ln (I_0/I)/\rho t$$

where I_0 and I are the beam currents in region L_2 in the absence and presence of laser irradiation, respectively, ρ is the photon density in this region, and t is the residence time of the ions in L_2. The value of σ_{IR} obtained from this equation are given in Table I. Their magnitudes lie in the range 10^{-19}–10^{-20} cm^2, with relative accuracy of ±20%. The absolute accuracy of the cross sections,

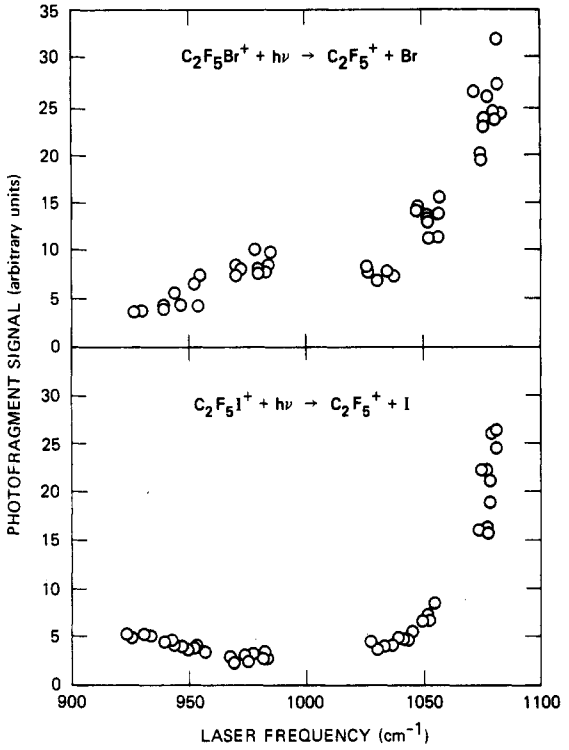

Figure 2. Relative photodissociation cross section for the production of $C_2F_5^+$ from $C_2F_5I^+$ (lower points) and $C_2F_5Br^+$ (upper points) as a function of photon energy. The large gaps in the data correspond to CO_2 laser tuning gaps.

however, is only to within a factor of 2, due to the uncertainty in measuring the laser power actually observed by the ions.

It should be emphasized that these photodestruction cross sections are phenomenological since only those ions in the beam which have internal energies within one IR photon of the dissociation limit or greater can be photodissociated. Consequently, the fact that the cross section for one ion is found to be larger than that of another may reflect only their difference in internal energy content rather than the ease with which the ions can absorb an IR photon and dissociate. Indeed, one expects an IR absorption cross section of order 10^{-17} cm^2. If an absorption cross section of this size is assumed, as much as 5% of the ion beam is populated in these highly excited states approximately 30 μs after the formation of the ions by 100-eV electron-impact ionization.

The RRKM model calculations followed well-known procedures.[14,15] Vibrational frequencies of the ions were taken to be the same as the neutral molecule which are accurately known in the case of CF_3I, and were estimated for the other molecules. Frequencies of the activated complexes were assigned by removing from the set of ground-state frequencies one mode having C-I stretching character, lowering the frequencies of two modes believed to have C-I bending character, and leaving all other frequencies unchanged. Density-of-state and number-of-state functions were obtained by direct count, where feasible, and by the steepest descents approximation[16,17] otherwise. Agreement of direct-count and approximate functions was excellent.

Results and Discussion

IR Photodissociation Spectra. It is a striking finding of this work that many of the ions show a strong wavelength dependence in the one-photon photodissociation process studied here. Figures 2–5 show spectra for a number of ions which have distinct wavelength dependence. Table I indicates a number of other ions whose wavelength dependences were observed but were found to show little variation across this wavelength region.

The two spectra in Figure 2 show essentially the same wavelength dependence for the one-photon dissociation of $C_2F_5Br^+$ and $C_2F_5I^+$. Both ions exhibit a strong absorption peak above 1080 cm^{-1}, although the actual line center may lie beyond the tuning range of the CO_2 laser. The somewhat larger scatter apparent in the $C_2F_5Br^+$ data is most likely due to the lower ion beam current levels for this species relative to the iodide, leading to a greater statistical variation in the photodissociation signal. Each

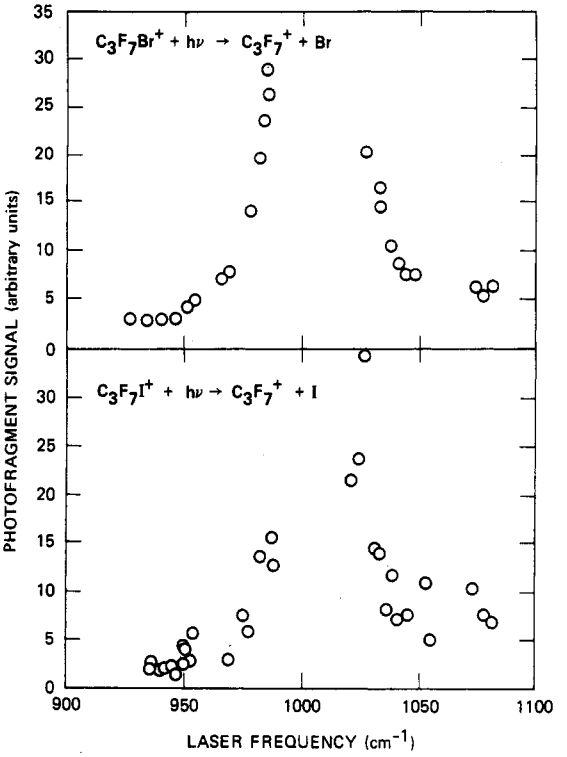

Figure 3. Relative photodissociation cross section for the production of $C_3F_7^+$ from $C_3F_7I^+$ (lower points) and $C_3F_7Br^+$ (upper points).

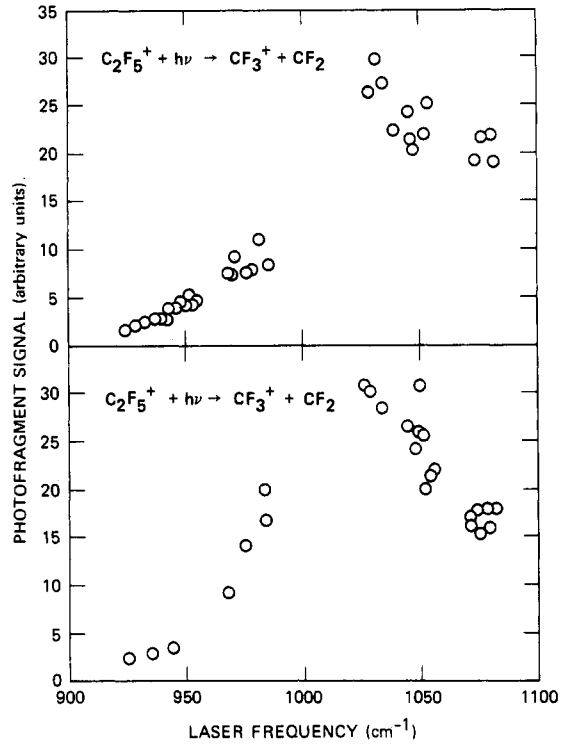

Figure 4. Relative photodissociation cross section for the production of CF_3^+ from $C_2F_5^+$. The $C_2F_5^+$ ions were formed by electron impact on C_2F_5I (lower points) and C_2F_6 (upper points).

(14) Forst, W. *Theory of Unimolecular Reactions*; Academic: New York, 1973.
(15) Robinson, P. J.; Holbrook, K. A. *Unimolecular* Reactions; Wiley: New York, 1972.
(16) Hoare, M. R.; Ruijgrok, T. W. *J. Chem. Phys.* **1970**, *52*, 113.
(17) Forst, W. *Chem. Rev.* **1971**, *71*, 339.

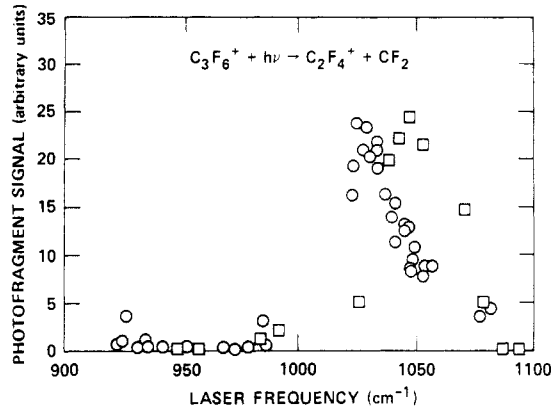

Figure 5. Relative photodissociation cross section for the production of $C_2F_4^+$ from perfluoropropylene ions, $C_3F_6^+$. The circles (○) are the present results, the squares (□) are from ref 19.

spectrum displays some reproducible secondary structure, the $C_2F_5Br^+$ having a small peak near 975 cm^{-1}, and the $C_2F_5I^+$ showing a broad increase below 950 cm^{-1}. Figure 3 contains the $C_3F_7Br^+$ and $C_3F_7I^+$ photodissociation yields as a function of wavelength. A fully resolved peak is apparent for both ions, with the bromide centered at 1000 cm^{-1} and the iodide possibly shifted to ~1020 cm^{-1}. Again, the fluctuations in the $C_3F_7I^+$ data resulted mainly from a lower parent ion beam current. The data in Figure 4 show the wavelength dependence for the photodissociation for $C_2F_5^+$ ions produced by electron impact on C_2F_5I in one case and on C_2F_6 in the other case. In each instance, the only observed ion product is CF_3^+, with the peak dissociation occurring near 1020 cm^{-1}. Both spectra exhibit a similar assymetry, having a noticeably larger absorption cross section toward higher energies. It also appears that the photodissociation spectrum of the $C_2F_5^+$ ions derived from C_2F_6 (lower points in Figure 4) is broader on the low-energy side than the corresponding C_2F_5I-derived ions. This difference appears to be reproducible and may reflect differences in the total internal energy content of the ions produced from the two parent molecules. Figure 5 presents the photofragment yield for the perfluoropropylene ion, $C_3F_6^+$, dissociation as a function of CO_2 laser frequency. A single narrow feature centered at 1030 cm^{-1} is observed for this ion, with essentially no dissociation found below ~990 cm^{-1}.

The origin of the observed strong wavelength dependence for IR absorption by highly vibrationally excited species has been treated theoretically by Hose and Taylor.[18] Their mode localization description accounts for a number of experimental observations including high-overtone C–H excitations, enhanced Raman spectroscopy, two-color MPD, as well as single-photon absorption in the quasi-continuum such as observed here.

Experimentally, similar peaking has been observed in other studies of IR excitation of polyatomic ions. In the visible/IR two-laser dissociation[7] of $C_6H_5I^+$, IR peaking is seen around 980 cm^{-1}. Distinct peaking is also observed in the IR multiphoton dissociation of ions; of interest is the $C_3F_6^+$ ion, for which Bomse, Woodin, and Beauchamp[19] found a peak at ~1043 cm^{-1}, as compared with the peak at 1030 cm^{-1} in the present work (see Figure 5). Similarly, Thorne and Beauchamp[10] find a peak in the multiphoton dissociation cross section of CF_3I^+ at 960 cm^{-1}, as compared to a value of 947 cm^{-1} found[9] for the single photon dissociation of this ion. These shifts reflect the difference in the two experiments: in the multiphoton experiments[19-21] photons appear to be absorbed by molecules in all states of excitation from the ground state up to E_0, while in the present work, all the ions are near E_0. The higher average of ions in the present work should, through the bond-stretching effects of vibrational anharmonicities, have the result of lowering slightly the observed vibrational peaks. The red shift of IR peaks in highly excited neutral molecule studies has been noted[22] and was invoked by Jarrold et al.[11] to explain the differing absorption peak positions observed in single-photon and multiphoton dissociation of CF_3I^+.

Fragmentation Rates and Energy Release. As noted earlier, an electrostatic analyzer is used to measure the laboratory kinetic energy distribution, $I(E)$, of the ion photofragments (see, for example, Figure 3, ref 9). The desired center-of-mass kinetic energy distribution is obtained from these measured spectra by differentiation with respect to energy, $dI(E)/dE$.[13] The average energy release values given here are calculated from the transformed distributions. Table I shows the values obtained for the kinetic energy released, and the fragmentation lifetime (from the (R_3/R_2) ratio), for a variety of ions. It should be noted that, in general, the average kinetic energy release accompanying metastable decomposition is measurably smaller than the corresponding value for photodissociation. These energy release values were determined for ions dissociating in region L_2; that is, the measurements were made under conditions where the second quadrupole was set to pass only fragment ions. In several cases, an additional energy release distribution was measured for ions which decayed in region L_3 and therefore had a correspondingly longer lifetime. These values are also given in Table I and are typically found to be larger than the corresponding L_2 result.

The ordering of the relative magnitude of the photodissociation and metastable decomposition lifetimes tends to be opposite that of the energy release results; that is, the IR-induced decomposition lifetimes are generally the smaller of the two. The typical magnitude of these lifetimes (even allowing for uncertainties associated with the calibration procedure) is in the microsecond range, making them several orders of magnitude longer than the nanosecond lifetimes normally found for multiphoton-excited molecules.[1] Even shorter lifetimes have been measured in studies of the one-photon IR-induced dissociation of weakly bound van der Waals molecules.[23] These photodissociation lifetimes in the 10^{-12}-s range were determined from the homogeneously broadened absorption profiles of various ethylene-containing species. The prompt decay mechanism at work in these latter systems appears different from the much slower mechanism which governs decay in the present ions. Recently, however, the unimolecular decay rate of multiphoton-ionized C_6H_6 was measured[24] and found to also be in the microsecond range.

The significance of these lifetime and energy release measurements is best considered in the context of a specific theoretical model for the dissociation processes, and the analysis below in terms of quasi-equilibrium theory gives good support to the appropriateness of this model.

Two cases were observed, $C_6F_6^+$ and CH_3F^+, in which the metastable decomposition branched to more than one product-ion species. As has usually (but not always) been found to be true for visible-wavelength photodissociation, the infrared-photon-induced decomposition in each of these cases yielded only a single product species.

Modeling by RRKM Theory. Quasi-equilibrium theory of unimolecular reactions, in the form known as RRKM theory,[14,15] has, properly formulated, been extraordinarily successful in accounting for qualitative and quantitative aspects of a great variety of polyatomic ion (and neutral) dissociation processes. This theoretical framework is entirely relevant to the dissociation process of multiphoton dissociation photochemistry,[1] and the present set of results provides a useful opportunity for testing its application to photochemically interesting ions undergoing IR photodissociation. The experimental data most important for this are the

(18) Hose, G.; Taylor, H. S. *Chem. Phys.* **1984**, *84*, 375.
(19) Bomse, D. S.; Woodin, R. L.; Beauchamp, J. L. *Advances in Laser Chemistry*; Springer: New York, 1978.
(20) Woodin, R. L.; Bomse, D. S.; Beauchamp, J. L. *J. Am. Chem. Soc.* **1978**, *100*, 3248.
(21) Woodin, R. L.; Bomse, D. S.; Beauchamp, J. L. In *Chemical and Biochemical Applications of Lasers*; Moore, C. B., Ed.; Academic: New York, 1979; Vol. 4.
(22) Rossi, M. J.; Barker, J. R.; Golden, D. M. *J. Chem. Phys.* **1982**, *76*, 406.
(23) Casassa, M. P.; Bomse, D. S.; Janda, K. C. *J. Chem. Phys.* **1981**, *74*, 5044.
(24) Kuhlewind, H.; Neusser, H. J.; Schlag, E. W. *J. Phys. Chem.* **1984**, *88*, 6104.

kinetic energy release, W_{IR}, and the photodissociation fragmentation rate, measured by the (R_3/R_2) ratio. The corresponding releases and rates for the metastable decompositions (when observed) are valuable for calibration and further testing of the quantitative applicability of RRKM methods in these molecules.

Three photodissociation reactions were chosen for detailed calculation as being representative of most of the trends and interesting features of the entire data set:

$$CF_3I^+ \rightarrow CF_3^+ + I \quad (1)$$

$$C_2F_5I^+ \rightarrow C_2F_5^+ + I \quad (2)$$

$$C_3F_7I^+ \rightarrow C_3F_7^+ + I \quad (3)$$

The theoretical considerations will focus on two questions raised by the data:

(1) Are the observed metastable and IR-induced decompositions, with their kinetic energy release values and (R_3/R_2) values, quantitatively consistent with the assumptions and results of RRKM theory, as worked out for the postulated one-photon IR dissociation process?

(2) It is perhaps counterintuitive that the W values are observed to increase in going from $C_2F_5I^+$ to $C_3F_7I^+$ (see Table II), as it is often expected that longer molecules will partition less of the available energy into translational energy of the fragments. Can this trend be understood?

Assumed Model. The following model of the events occurring in the ion beam will be adopted and combined with the usual assumptions of RRKM calculations:

(1) The electron-impact ion source provides the ions with a wide range of internal energies. The distribution of internal energies (energy deposition function) will be taken as being uniform over the relevant range of approximately 1000 cm^{-1} on either side of the dissociation threshold E_0. This assumption is ad hoc but is consistent with the fact that both spontaneous decay and single IR photon dissociation occur.

(2) During the flight in L_1 from the source to the first quadrupole (duration ~ 60 μs), those ions with energies well above E_0 dissociate and are lost from the beam, so that the distribution of ion internal energies entering L_2 is truncated above a certain value.

(3) During the flight in L_2 (typically 10 μs), some ions dissociate spontaneously, with energy release W_{meta}. Some ions absorb an IR photon of energy 1000 cm^{-1}, with a probability which is independent of their internal energy and may dissociate in L_2 with energy release W_{IR}.

(4) During the flight in L_3 (typically 30 μs), a small number of additional metastable ions dissociate; also, some of the photoexcited ions surviving transit through the second quadrupole dissociate. The rates of both metastable and IR-induced dissociation in L_2 and L_3 may be compared, giving $(R_3/R_2)_{meta}$ and $(R_3/R_2)_{IR}$, respectively.

(5) During the flight between the quadrupoles, ions may be excited by collisions with neutrals and subsequently dissociate as light-independent, pressure-dependent metastables with kinetic energy release W_{CID}.

Given the assumptions of this model, along with sufficient information about the ion and its dissociative activated complex, the rates and energy releases of the processes in steps 3 and 4 can be evaluated within the RRKM framework. However, the collision-induced process 5 cannot be evaluated without the added information of the collision energy input to the ion, and it is better to consider W_{CID} values as giving insight into the very interesting question of collisional energy transfer.

Calculations. Not all of the fragmentation threshold energies are well-known for the ions of interest. In the case of CF_3I^+, the photoionization appearance threshold for CF_3^+ production from trifluoromethyl halides has been determined,[25] yielding a fragmentation energy of 8400 cm^{-1} for ground electronic state CF_3I^+. Dissociation of the corresponding $^2E_{1/2}$ ionic species reduces this value to ~ 3700 cm^{-1}. Within very wide limits, however, the threshold for this ion has no effect on the analysis and conclusions drawn here.

In the case of $C_2F_5I^+$, an electron impact measurement[26] of the $C_2F_5^+$ appearance potential suggests a threshold of 8700 cm^{-1} for reaction 2, but in view of the known unreliability of electron impact methods, this value must be viewed with caution. Accordingly, it was assumed that the fragmentation of metastable $C_2F_5I^+$ ions observed in these experiments is governed by RRKM kinetics, and the threshold energy was adjusted so that the calculations yielded the observed metastable fragmentation rate (i.e., $(R_3/R_2)_{meta}$). The value of 7700 cm^{-1} obtained is not far from the electron impact value.

No data appear to exist on the threshold of reaction 3, for $C_3F_7I^+$, so again this was treated as an adjustable parameter. A value of 7400 cm^{-1} gave the best overall results, but none of the calculated values are very sensitive to this parameter, which could be varied by several hundred of even a thousand cm^{-1} without degrading the RRKM fit.

CF_3I^+. The conclusions for this ion are clear: dissociation is rapid ($>10^8$ s^{-1}) for all energies significantly above E_0. Therefore, no CF_3I^+ ions are expected to reach the interaction region with internal energy above E_0, and any ion photoexcited above E_0 will dissociate promptly. The average internal energy of photodissociating ions is thus about $E_0 + h\nu/2$ cm^{-1}. The standard method of calculating the kinetic energy release assumes that the energy partitioning between the internal coordinates and the reaction coordinate in the transition state carries over to the dissociated products; this is embodied in eq 10-83 of ref 14 and yields a predicted W_{IR} of 14 meV. A recent reformulation of RRKM theory by Klots[27] yields an alternative energy release formula for Langevin-model ion–molecule systems, given in useful form in eq 5 of ref 15; this yields a predicted W_{IR} of 9 meV.

The rapid decay rate is consistent with our observation of a lifetime $\ll 1$ μs, and the calculated energy release is in reasonable agreement with the measured value (see Table II). Thus a QET description appears to be reasonable for this dissociation. This is similar to the behavior of CH_3I^+, for which Mintz and Baer[28] found that their results at excitation levels up to 1.7 eV above threshold were reproduced with reasonable accuracy by Klot's theory. As they noted, the interaction potential for the separating fragments in CH_3I^+ (and similarly for CF_3I^+) dissociation is likely to be correctly described by a simple ion-induced dipole potential with no exit-channel barrier. As a result, one would not expect a priori to observe any nonstatistical lifetime or energy release distributions of the type found by Wolf and Hase[29] in a calculation using classical trajectories for triatomic dissociation on empirical energy surfaces with early exit-channel barriers. This same theoretical study also showed that, for simple cases where either a late barrier or no exit barrier is present, one finds that both the lifetime distribution as well as the fragment energy release distributions are statistical, i.e., intrinsically RRKM.

$C_2F_5I^+$. Because of their rapid dissociation, there is low probability of $C_2F_5I^+$ ions reaching L_2 with much energy above E_0. Ions having enough energy to populate the first excited state of the activated complex (assumed to be a torsional motion at 40 cm^{-1}) will be strongly depleted relative to ions below this energy, so that metastable decompositions in L_2 and L_3 should arise predominantly from ions in the ground vibrational state of the activated complex, that is, with 0–40 cm^{-1} of excitation above E_0. As indicated in Table II, the kinetic energy release calculated on this basis for metastable decomposition is ~ 3 meV, which is not far from the observed value of 4.5 meV. (This calculation is rather uncertain, since it depends strongly on the characteristics of the low-frequency torsional or internal-rotational mode of the activated complex or of the $C_2F_5^+$ product, which are very poorly known.)

(25) Berman, D. W.; Bomse, D. S.; Janda, K. C. *J. Chem. Phys.* **1981**, *74*, 5044.

(26) Hsieh, T.; Hanrahan, R. J. *Int. J. Mass Spectrom. Ion Phys.* **1977**, *23*, 201.

(27) Klots, C. E. *Adv. Mass Spectrom.* **1974**, *6*, 969.

(28) Mintz, D. M.; Baer, T. *J. Chem. Phys.* **1976**, *65*, 2407.

(29) Wolf, R. J.; Hase, W. L. *J. Chem. Phys.* **1980**, *72*, 316.

As noted above, the $(R_3/R_2)_{meta}$ ratio was treated as an adjustable parameter in choosing E_0, so this value and τ_{meta} necessarily agree with experiment.

In photodissociation, the ions will have a spread of internal energies above E_0, because of their spread of energies prior to photon absorption, and in addition because they can absorb the photon at any point along L_2. Thus, the calculations involve numerical integrations over distributions in energy and position of absorption along L_2. Both the kinetic energy release and lifetime values calculated in this manner are in good agreement with the experimentally observed results.

$C_3F_7I^+$. With this ion, the situation changes qualitatively, as the higher heat capacity brings the ions into a regime where the typical metastable ion retains several hundred cm^{-1} of energy above E_0 into L_2, and where only the more energetic of these excited ions dissociate before reaching the detector, necessitating a more detailed calculation. According to the RRKM rates, ions up to about 500 cm^{-1} internal energy above threshold would survive into L_2, but most ions more energetic than this would dissociate before reaching L_2. Accordingly, the metastable ions dissociating in L_2 will have energy close to 440 cm^{-1}, giving an average kinetic energy release W_{meta} of 10 meV (9 meV using Klots' expression).

W_{IR} was calculted on the assumption that the ions in L_2 absorb a photon to give a uniform distribution of internal energies from 0 to 1500 cm^{-1}. Of these the ions with $\geq$900 cm^{-1} are likely to decompose in L_2, while those below 900 cm^{-1} are likely to survive through L_2. Assigning an average of 1200 cm^{-1} to the decomposing ions leads to a kinetic energy relese W_{IR} of 21 meV (15 meV using Klots' expression).

Calculating the lifetimes for this ion requires a numerical integration in which the number of ions dissociating at each point in L_2 and L_3 is determined, summing over the distribution of internal energies of the ions, and also (for the calculation of $(R_3/R_2)_{IR}$) summing over all the positions along L_2 where the ions can absorb a photon. Finally summing over L_2 and L_3 gives the ratios $(R_3/R_2)_{meta}$ and $(R_3/R_2)_{IR}$, and the corresponding τ values.

As shown in Table II, the agreement with experiment is quite satisfactory for all the $C_3F_7I^+$ numbers.

Conclusions about the QET Comparison. The principal conclusions of this analysis are the following

1. The dissociation rates and average kinetic releases for these three ions are well accounted for within the RRKM point of view, considering both metastable decomposition and IR-induced dissociation, and using entirely reasonable values of the RRKM parameters without special, nonstatistical features of the dissociation mechanism.

2. The increase in W values with increasing size of the molecule falls naturally out of the calculations and is a consequence of the ability of larger ions to carry substantial amounts of internal excitation into the photon-interaction region without spontaneously dissociating. In effect, the average large ion is much "hotter" than the average small ion at the moment of dissociation in L_2 or L_3.

One should view as significant in these conclusions the finding that the present observations are easily accounted for by the RRKM mechanism with reasonable input parameters (dissociation energies, frequencies of the energized ion and the activated complex, energy distribution of the ions emerging from the source). As with most such comparisons where the dissociation thermochemistry and the characteristics of the ions are not very well-known, the detailed agreement of experiment and theory is unimportant. As long as a fragmentation process is in general agreement with a QET mechanism, it is normally possible to tinker with the RRKM parameters to make the quantitative agreement as good as desired. This tinkering process was not carried very far in the present case, and the quantitative agreement could easily be improved, but this would have little significance. With the exception of W_{meta} for $C_2F_5I^+$, the calculated values are relatively insensitive to parameter changes (considering variations of 20 or 30% in either calculated or measured values to have little significance).

It is not necessary to interpret these results in terms of detailed potential surfaces and dissociation dynamics, at least at the level at which the results are aggregated into average kinetic energy release and phenomenological dissociation lifetimes. We have not attempted to evaluate the success of a QET model at a higher level of detail, for instance, by looking at distributions of kinetic energies and dissociation rates. The success of the theory at the present level argues against dissociation from repulsive electronic potential surfaces, and against drastic isolation of a small group of quantum states with respect to energy randomization.

Conclusions

The wavelength-dependent single-photon dissociation of highly vibrationally excited polyatomic ions first observed with CF_3X^+ (X = I, Cl, Br) has now been seen to occur in a wide variety of molecular ions. In addition, many of the ions studied here also exhibit metastable decomposition with lifetimes in the 20–100-μs range. The decomposition lifetimes estimated for the photodissociation process are in general significantly smaller than the corresponding metastable lifetimes. For those cases where the fragment kinetic energy distributions were measured, the faster photodissociation mechanism always yielded a larger average energy release than the slower metastable dissociation.

Acknowledgment. This work was supported in part by the Office of Naval Research. Support of the research of R.C.D. during the period when this work was carried out is acknowledged from donors of the Petroleum Research Fund, administered by the Americal Chemical Society, The National Science Foundation, and the U.S. Air Force Geophysics Laboratory.